Published in final edited form as:
Atherosclerosis. 2012 April ; 221(2): 350–358. doi:10.1016/j.atherosclerosis.2011.10.005.

Selective improvement in renal function preserved remote myocardial microvascular integrity and architecture in experimental renovascular disease

Victor H. Urbieta-Caceres[a], **Xiang-Yang Zhu**[a], **Kyra L. Jordan**[a], **Hui Tang**[a], **Kyle Textor**[a], **Amir Lerman**[b], and **Lilach O. Lerman**[a,b]

[a]The Divisions of Nephrology and Hypertension, Mayo Clinic, Rochester, MN 55905, United States

[b]Cardiovascular Diseases, Mayo Clinic, Rochester, MN 55905, United States

Abstract

Aim—Atherosclerotic renovascular disease (ARVD) may impair renal function and increase cardiovascular morbidity and mortality, but the mechanism by which ARVD impacts cardiovascular function is unclear. We tested the hypothesis that preservation of renal function can reverse cardiac dysfunction in ARVD.

Methods and results—Endothelial progenitor cells (EPC) were injected intra-renally (ARVD + EPC) after 6 weeks of swine ARVD (concurrent hypercholesterolemia and renovascular hypertension), and single kidney function and myocardial blood-flow and microvascular permeability (MP) responses to adenosine were assessed using CT 4 weeks later. Myocardial microvascular density was evaluated by micro-CT. Inflammation and oxidative-stress were assessed in kidney venous and systemic blood samples. Normal and untreated ARVD pigs served as controls. Blood pressure was similarly increased in ARVD and ARVD + EPC. Compared to normal, ARVD showed lower glomerular filtration rate, elevated renal vein and systemic oxidized LDL (ox-LDL), aldosterone, uric acid, isoprostanes, transforming growth factor (TGF)-, and interleukine-6. Renal vein ox-LDL and TGF-showed a positive gradient across the stenotic kidney, indicating increased renal oxidative stress and fibrogenic activity. Furthermore, ARVD impaired myocardial blood-flow and MP response to adenosine, decreased microvascular density, and induced myocardial fibrosis. Improvement of renal function in ARVD + EPC decreased systemic aldosterone, inflammation, and oxidative stress, and improved myocardial microvascular integrity and density.

Conclusion—Selective improvement in renal function, which reduced renal and systemic oxidative stress and inflammation, preserved remote myocardial microvascular function and architecture, despite enduring hypertension. These findings underscore functionally important cardiorenal crosstalk possibly mediated by renal injury signals.

Keywords

Atherosclerosis; Inflammation; Microcirculation

Correspondence: Lilach O. Lerman, MD, PhD, Division of Nephrology and Hypertension, Mayo Clinic, 200 First Street SW, Rochester, MN 55905. Fax: (507)-266-9316, Phone: (507)-266-9376, lerman.lilach@mayo.edu.

Introduction

The prevalence of chronic kidney disease (CKD), which currently is 13% [1], is on the rise in the US adult population. Morbidity and mortality in CKD patients due to cardiovascular events are significantly higher than in the general population [2], and increase with decreasing glomerular filtration rate (GFR) [3,4]. In addition to decreased GFR, hypertension and atherosclerosis are also independent risk factors for both cardiovascular disease and CKD, and particularly characterize atherosclerotic renovascular disease (ARVD). ARVD may lead to CKD, but constitutes an independent risk factor for cardiovascular morbidity and mortality [5]. However, the mechanism by which declines in kidney function signal and lead to cardiac impairment remain unclear.

Several mechanisms have been proposed to mediate the crosstalk between the kidney and heart, including the sympathetic nervous system, the renin–angiotensin–aldosterone system, oxidative stress, or inflammation, which are all activated in CKD and may alter microvascular function in both the renal and cardiac microcirculations. However, the link to the kidney has often been indirect. Renal dysfunction is associated with increased levels of inflammatory biomarkers such as interleukine-6 (IL-6) [6], and we have previously shown that it is also associated with myocardial microvascular dysfunction in humans [7] and impairs myocardial microvascular architecture and integrity in experimental renovascular hypertension [8]. Indeed, myocardial microvascular dysfunction in ARVD may be secondary to co-existing hypertension, humoral factors (such as circulating oxidative or inflammatory mediators), or to a yet unknown direct effect of decreases in GFR. However, the interaction between renal dysfunction and cardiovascular function remains poorly understood.

Few therapeutic interventions afford selective direct local repair of the kidney alone. Endothelial progenitor cells (EPC) play a major role in vascular repair, and we have previously shown that they restore the hemodynamics and function of the ischemic kidney and attenuate renal remodeling, without affecting systemic hypertension [9,10]. Nevertheless, the potential of selective renal functional improvement to reverse myocardial microvascular dysfunction and remodeling is unclear. Therefore, this study tested the hypothesis that improvement in renal function using selective intra-renal administration of EPC in a swine model of ARVD would decrease systemic levels of noxious humoral factors and rescue myocardial microvascular function.

Materials and methods

This study was approved by Mayo Clinic Institutional Animal Care and Use Committee, following the Guide for the Care and Use of Laboratory Animals published by the United States National Institutes of Health. Twelve domestic pigs (35–40 kg) were fed with 2% cholesterol and 15% lard by weight (TD93296, Harlan Teklad, Madison, WI) for 6 weeks, to induce pre-existing early atherosclerosis. At 6 weeks, each animal was anesthetized with intramuscular ketamine (20 mg/kg) and xylazine (2 mg/kg), intubated, ventilated, and anesthesia was maintained with 1.5% isoflurane inhalation. Under sterile conditions and fluoroscopic guidance, a 7.0 mm PTCA balloon with a mounted copper wire coil was then advanced through the guide catheter into the left renal artery, and engaged in the proximal-middle section of the renal artery. The balloon was inflated once to high pressure (6 atm), resulting in expansion of the coil to full balloon diameter, and then deflated and removed, leaving the coil in place [11,12]. A telemetry catheter was then secured in the left femoral artery for monitoring daily blood pressure, including 24 h systolic, diastolic, and mean arterial pressure (MAP), daytime (8 am–10 pm) and nighttime (10 pm–8 am) [13] MAP, and the high cholesterol diet and ARVD constellation continued for another 10 weeks. Six

weeks after induction of renal artery stenosis, animals were randomized into two groups: sham-treated (ARVD, n = 6) or treated with a single intra-renal infusion of pre-labeled autologous EPC (ARVD + EPC, n = 6). EPC were obtained from peripheral mononuclear cells, which were isolated, expanded, and delivered to the stenotic kidney of the same ARVD + EPC pig [9,10]. Six additional pigs were used as normal controls.

The severity of stenosis was determined by renal angiography, as previously described [9,11,12]. For this purpose, animals were anesthetized with intramuscular ketamine (20 mg/kg) and xylazine (2 mg/kg), intubated, and ventilated. Anesthesia was maintained with ketamine (0.2 mg/kg/min) and xylazine 0.03 mg/kg/min), and the degree of stenosis assessed fluoroscopically. Then in treated pigs EPC were injected through an 8F catheter in the stenotic renal artery [9,10].

Four weeks after EPC infusion, in vivo multi-detector computed tomography (MDCT) were conducted in all pigs under the same anesthesia to evaluate stenotic and contralateral kidneys GFR, stenotic kidney blood-flow, as well as cardiac function, structure, and microvascular function, including myocardial microvascular permeability (MP) and blood-flow. A pigtail catheter in the right atrium served for contrast media injection, and a side-arm for adenosine infusion. Blood samples were collected from the inferior vena cava for measurement of plasma renin activity (PRA, GammaCoat PRA kit; DiaSorin, Inc., Stillwater, Minnesota, USA), aldosterone, endothelin-1 (ET-1), and total cholesterol. Inflammation was assessed by tumor necrosis factor (TNF)-α and interleukine-6 (IL-6); oxidative stress by circulating PGF-2α isoprostanes, uric acid, and oxidized (ox)-LDL, and fibrogenic activity by levels of transforming growth factor (TGF)-β. Blood samples were also collected from the bilateral renal veins for measurement of PRA, ox-LDL, uric acid, PGF-2α isoprostanes, IL-6, and TGF-β. Urine samples were collected during the CT study by supra-pubic aspiration for protein measurement.

A few days after completion of the in vivo studies, the pigs were euthanized using an intravenous lethal dose of sodium pentobarbital (100 mg/kg), and left ventricle (LV) tissue harvested for in vitro studies. Cardiac tissue was frozen or preserved in formalin, and another segment prepared for micro-CT studies and evaluation of microvascular density.

In vivo CT studies

After angiography, in vivo MDCT (Somatom Sensation-64, Siemens Medical Solution, Forchheim, Germany) flow studies were performed for assessment of the stenotic and contralateral singlekidney blood flow and GFR, as previously detailed [9,11,12]. Total renal GFR was obtained as the sum of right and left kidney GFR.

Cardiac microvascular function was evaluated by myocardial MP and blood-flow responses to intravenous adenosine [8,14]. Mid LV levels were selected and a 50-s flow study performed at endexpiration after a bolus injection of the contrast medium iopamidol (Isovue-370, 0.33 ml/kg over 2 s) into the right atrium. The same procedure was repeated after a 15-min rest during a 5-min intravenous infusion of adenosine (400 μg/kg/min). Two parallel 6-mm thick sections of the heart were studied with a full-scan reconstruction. In addition, the LV was scanned 20 times throughout the cardiac cycle during iopamidol infusion for measurements of cardiac systolic and diastolic functions and LV-muscle mass (LVMM) [8,15–17].

EPC preparation, delivery and engraftment Peripheral blood (100 ml) was drawn 3 weeks (for late EPC) and 1 week (for early EPC) before injection, as described previously [9]. Briefly, mononuclear cells obtained from systemic blood were cultured in endothelial media (EGM-2 plus EGM-2 Singlequot medium, Lonza, Walkersville, MD). Before delivery the

cells were labeled with a fluorescent membrane dye (CM-DiI) and kept in 10 ml PBS on ice. An equal blend of early and late EPC was infused (10^6 cells/ml) into the stenotic renal artery 6 weeks after ARVD induction. EPC retention rate were estimated from cells observed in the stenotic kidney sections, as previously described [9,10]. CM-DiI fluorescence was examined to evaluate the retention and location of EPC.

2.3. Cardiac CT data analysis

The images were analyzed with the Analyze® software package (Biomedical Imaging Resource, Mayo Clinic, Rochester, MN). For cardiac systolic function, the LV endocardial and epicardial surfaces were traced at end-diastole and end-systole. LV ejection fraction, stroke volume, end-diastolic volume (EDV), and LVMM were calculated as previously described [16–18]. For diastolic function, the volume of the entire LV cavity throughout the cardiac cycle was plotted as time–volume curves. Early (E) and late (A) LV filling rates were obtained from the positive slopes of the curve and E/A ratio calculated, as described [8,17].

In addition, regions of interest were manually traced at end diastole in the cardiac anterior wall. The time–density data were then used to assess myocardial blood-flow (perfusion × LVMM) based on the indicator-dilution technique, as previously shown [15,17], and MP (arbitrary units [AU]) based on the Patlak graphical analysis method [8,14].

Micro-CT study

Micro-CT was used to evaluate myocardial microvascular architecture, as previously shown [8,9,15–17]. Briefly, the heart was excised, the microvessels fully relaxed during overnight refrigeration, the left anterior descending artery perfused with a contrast agent (Microfil MV122, Flow Tech, Carver, MA) under physiological pressure (100 mm Hg), and a myocardial segment (≈2 cm × 1 cm × 1 cm) was scanned. Images were digitized for reconstruction of 3-D volume images, and analyzed using AnalyzeTM in 7-slices obtained at equal intervals to calculate the subepicardial, subendocardial, and trans-mural microvascular density.

Histology

Fluorescence of CM-DiI was examined to localize pre-labeled EPC in frozen sections of the heart and kidney [9].

Trichrome and Sirius-Red staining was performed in 5 J-m paraffin cardiac cross-sections to assess fibrosis. Quantitative analysis utilized a computer-aided image analysis program (MetaMorph® , Meta-Imaging Series-6.3.2, Molecular Devices, Sun- nyvale, CA) to calculate the fraction of positive trichrome stain in 10–15 random fields per slide [16–18]. The Sirius red sections were examined under polarized light microscopy to detect type- I collagen fibers [17,19], and their fraction was quantified using MetaMorph®.

Plasma measurements

Systemic or renal vein plasma levels of TNF-cx, IL-6 (Quantikine® , R&D, Minneapolis, MN), uric acid, aldosterone, ET-1, PGF-2cx iso- prostanes (Cayman chemical/Ann Arbor, MI), Ox-LDL (Alpaco, Salem, NH) and TGF-(3 (R&D Systems) were determined by ELISA, as previously described [8,15,20]. Gradients across the stenotic kidney were calculated as: (level in vein draining the stenotic kid- ney − systemic level) × renal blood flow.

Statistical analysis

Results are presented as mean ± SEM. One-way analysis of variance (ANOVA) (in normally distributed data) or Kruskal–Wallis test was used to evaluate differences among the groups, followed by an unpaired t-test with the Bonferroni or Welch's correction, while paired Student's t-tests or Wilcoxon matched-pairs test were used to detect changes within groups (adenosine vs. baseline). $p \leq 0.05$ was considered significant.

Results

Blood pressure (systolic, diastolic, average daily MAP, and daytime vs. nighttime MAP), the degree of stenosis, and cholesterol levels were all similarly and significantly greater in ARVD and ARVD + EPC animals compared to normal (Table 1), and were unaffected by intrarenal injection of EPC (Fig. 1). MAP dropped during the night in all groups. Urinary protein levels were similar among the groups.

The stenotic ARVD kidney was smaller compared with both normal and contralateral kidneys (Table 2). Functionally, both absolute GFR and GFR indexed to cortical volume in ARVD were significantly lower than normal and contralateral kidneys, and significantly improved with EPC treatment (p = NS vs. normal, $p = 0.006$ vs. ARVD). Similarly, renal blood flow and perfusion were significantly decreased in ARVD, but significantly improved in ARVD + EPC (Table 2).

Cardiac function and microvascular function

Stroke volume and cardiac output were similar among the groups. E/A ratio significantly decreased in both ARVD and ARVD + EPC compared to normal ($p = 0.0002$), suggesting diastolic dysfunction. However, in ARVD + EPC, E/A ratio significantly improved compared to untreated ARVD ($p = 0.03$, Table 1). EDV was decreased in ARVD ($p = 0.001$ vs. normal), as may be observed in hypertension with LV hypertrophy [21]. LVMM increased in ARVD and ARVD + EPC compared to normal ($p < 0.001$ and $p < 0.01$, respectively), yet in ARVD was also higher than ARVD + EPC ($p < 0.001$), indicating greater myocardial hypertrophy.

Basal anterior cardiac wall myocardial blood-flow was not different among the groups (Fig. 1B). Adenosine induced a significant increase in myocardial blood-flow in normal and ARVD + EPC pigs ($p = 0.03$ and $p = 0.05$ vs. baseline, respectively, Fig. 1B), but not in ARVD, suggesting microvascular dysfunction that was significantly improved in ARVD + EPC.

Patlak-derived basal MP in the anterior LV wall was significantly and similarly increased in ARVD and ARVD + EPC compared to normal (Fig. 1C, $p = 0.01$ for both). In response to adenosine, MP significantly increased only in ARVD, while in normal and ARVD + EPC MP remained unaltered during adenosine (Fig. 1C).

Systemic biomarkers

Plasma levels of the inflammatory markers TNF-α (Table 1) and IL-6 (Fig. 2A) were elevated in ARVD ($p < 0.04$ vs. normal) and decreased in ARVD + EPC ($p < 0.04$ vs. ARVD), but only IL-6 completely normalized, while TNF-α remained higher than normal ($p < 0.001$, Table 1).

Systemic levels of the oxidative stress markers PGF2α-isoprostanes and uric acid significantly increased in ARVD compared to normal ($p = 0.009$ and $p = 0.0002$, respectively), and both decreased in ARVD + EPC compared to ARVD ($p = 0.04$ for both,

Fig. 2A), but remained higher than normal (p = 0.02 and p = 0.03, respectively, Fig. 2A). On the other hand, systemic ox-LDL that was elevated in ARVD (p = 0.01 compared to normal) declined in ARVD + EPC (p = 0.03 vs. ARVD, p = 0.12 vs. normal, Fig. 2A).

There was no significant difference among the groups in systemic (Table 1) or renal vein (data not shown) PRA. Contrarily, circulating ET-1 increased in both ARVD and ARVD + EPC compared to normal (p = 0.0001 and p = 0.0004, respectively), although in ARVD + EPC it was lower than ARVD (p = 0.01, Table 1). Systemic levels of aldosterone increased only in ARVD (p = 0.04 vs. normal, p = 0.05 vs. ARVD + EPC, Table 1), as did TGF-β (p = 0.02 vs. normal and ARVD + EPC, Fig. 2).

Biomarkers levels in the renal veins

PGF2α-isoprostanes were similarly increased in both kidneys of ARVD and ARVD + EPC compared to normal (p < 0.01 for both, Fig. 2B and C). Ox-LDL in the renal veins of both kidneys was also significantly elevated in ARVD compared to normal and ARVD + EPC (Fig. 2B and C), but in ARVD + EPC renal vein ox-LDL was not significantly different than normal (p = 0.2). Similarly, uric acid levels significantly increased in the vein of both kidneys and decreased in ARVD + EPC, suggesting increased renal oxidative stress in ARVD that declined in ARVD + EPC. However, the decrease in uric acid levels after EPC was slightly greater in the vein of the stenotic (p = 0.03 vs. ARVD, Fig. 2B) than the contralateral (p = NS vs. ARVD) kidneys. IL-6 was undetectable in normal pigs and in the renal veins of ARVD + EPC pigs, and its elevation in ARVD (to 228 ±172 pg/ml) has not reached statistical significance. TGF-β in the stenotic kidney vein increased in ARVD compared to normal and ARVD + EPC (p = 0.03 and p = 0.04, respectively, Fig. 2B), but declined to normal levels (p = 0.3) in ARVD + EPC, and remained unchanged in the vein of the contralateral kidney.

Comparison of biomarkers levels in the renal veins and the systemic circulation

Renal vein PGF2α-isoprostanes in both kidneys were similar to their systemic levels in normal (p = 0.4) and ARVD + EPC pigs (p = 0.9). In ARVD the systemic levels were higher than in both renal veins and their gradient was negative (p = 0.04, Fig. 2C and D), suggesting that PGF2 a-isoprostanes did not originate but were cleared in the kidney. Similarly, although the systemic and renal vein levels of uric acid were not different in any group, it showed a negative gradient across the stenotic kidney.

Renal vein levels of ox-LDL were significantly higher in all the groups compared to systemic blood (positive gradients). The gradient across the stenotic kidney was significantly larger than normal in the ARVD kidney (Fig. 2C and D), indicating greater oxidation of LDL. In ARVD + EPC this gradient was similar to normal (p = 0.46). The contralateral kidney vein also showed increased ox-LDL levels. The systemic and renal vein levels of IL-6 were low in both normal and ARVD + EPC pigs, as observed in healthy humans [22], while in ARVD IL-6 was detectable in all sites but significantly elevated only in the systemic circulation and substantially decreased in ARVD + EPC. Importantly, TGF-β levels in the vein of the stenotic kidney were higher than its systemic levels (p = 0.01, Fig. 2B and D), while in the contralateral kidney it was similar among the groups (Fig. 2C) indicating specific release of TGF-β from the stenotic ARVD kidney.

Microvascular density

Epicardial and transmural density of microvessels (diameters 20–200 μm) was selectively decreased in ARVD compared to both normal (all p = 0.002 vs. normal, Fig. 3A and B) and ARVD + EPC (p = 0.04 and p = 0.03, respectively, Fig. 3A and B), suggesting that vascular loss was prevented with EPC improvement in renal function.

Cardiac remodeling

EPC retention rate in the kidney was ~10–15% (approximately 12–15 cells per field), and abundant EPC were evident at the vascular, tubular, and glomerular compartments. In the myocardium EPC were rarely observed (1–2 EPC every 10 fields, Fig. 4A and B). Myocardial interstitial fibrosis observed in ARVD ($p < 0.01$ vs. normal) as trichrome and Sirius-Red staining was ameliorated in ARVD + EPC ($p < 0.01$ vs. ARVD, Fig. 4C and D).

Discussion

The present study shows that despite sustained hypertension, restoration of ischemic kidney function by a single intrarenal infusion of EPC in ARVD improved myocardial microvascular integrity and architecture and prevented cardiac interstitial fibrosis four weeks later, in association with improvement in diastolic function. Attenuated cardiac injury was accompanied by reduced renal and systemic oxidative stress, inflammation, fibrotic mediators, and vasoactive substances. This study therefore supports the notion that circulating mediators contribute to the crosstalk between the kidney and heart during renal dysfunction.

Both ARVD and decreased GFR predict cardiovascular morbidity and mortality, independent of other cardiovascular risk factors [4,5], and coronary vascular dysfunction predicts cardiovascular events [23]. Furthermore, coexistence of cardiac and renal dysfunction is associated with poor prognosis [24], while kidney transplantation in patients with congestive heart failure and end-stage renal-disease increases left ventricular ejection fraction, suggesting cardiorenal crosstalk [25]. However, the nature of the interaction of the heart and kidney remains poorly understood. Our previous studies demonstrated that renovascular hypertension impaired myocardial microvascular function, blunted myocardial blood-flow responses to challenge [15,18], and induced myocardial microvascular remodeling, in association with increased plasma levels of TNF-α and oxidative stress [16,17]. Furthermore, we have recently shown in humans a correlation between decreased GFR and myocardial microvascular dysfunction [7], and additional studies associated inflammation, oxidative stress, and renal and cardiac dysfunction [26,27]. However, the link among them is difficult to trace back specifically to the kidney without an intervention capable of selectively improving kidney function without conferring additional systemic benefits that might directly affect the heart, such as a decrease in blood pressure. Clinical experience and our previous studies have shown that while percutaneous transluminal renal stenting (PTRS) can decrease blood pressure in selected individuals, it does not consistently improve renal function in subjects with ARVD [28]. On the other hand, we have shown that a single intrarenal infusion of autologous EPCs in experimental chronic RAS and ARVD improved stenotic kidney function [9,10], thanks to their paracrine effects (e.g., growth factor secretion) and engraftment in renal structures to replace injured cells. Because these momentous outcomes are achieved in the absence of a significant effect on blood pressure, they may allow discerning the role of the kidney in the cardiorenal crosstalk. Taking advantage of these properties, the current study thus extends our previous observations to show that cardiac alterations in CKD are partially mediated by kidney-derived humoral factors, and underscores the ability of targeted augmentation of renal function to improve the systemic milieu and thereby cardiac microvascular function and structure.

In this study we assessed predominant inflammatory, oxidative, and vasoactive mediators that are stimulated in ARVD and might induce cardiac injury. To assess their possible role as kidney injury signals, we measured their levels in the systemic circulation and the veins draining both the stenotic and contralateral kidneys. Central venous levels served as a surrogate for arterial levels for calculation of gradients across the kidney.

An important potential mediator of renal and cardiac injury in hypertension and ARVD could be the renin–angiotensin–aldosterone system [16,17,20,29]. In experimental ARVD PRA increases transiently [29], while in the chronic setting low levels of angiotensin II suffice to sustain hypertension. Systemic PRA levels in our pig model were not elevated at the time of observation, reflecting the relatively chronic stage of ARVD. Nevertheless, the local renin–angiotensin system might have remained activated, and the AT1 receptor, which is upregulated in our model [8], contributes to cardiac hypertrophy and fibrosis [30]. Furthermore, circulating aldosterone levels were elevated in ARVD, consistent with our previous study [8]. Aldosterone may induce oxidative stress, inflammation, and fibrosis [31], and might increase ET-1 synthesis [32], LVMM, and cardiovascular risk in patients with hypertension [33]. Therefore, the decrease in cardiac remodeling that we observed in ARVD + EPC can be partly attributable to decreased activation of the renin–angiotensin–aldosterone system.

We observed that isoprostanes levels in ARVD were similarly decreased in both renal veins compared to peripheral blood, and showed a negative gradient across the stenotic kidney, confirming renal clearance of isoprostanes produced in the systemic circulation [34]. Isoprostane generation was likely triggered mainly by systemic hypertension and hypercholesterolemia, because they remained elevated following improvement in stenotic kidney function. Uric acid showed a similar pattern, but EPC were more effective in improving its renal vein levels, implying that declined renal function contributed to systemic uric acid production [35]. However, these patterns argue against isoprostanes or uric acid as chief stenotic–kidney-derived mediators of distant cardiac injury.

The major plausible culprits that were elevated in the renal vein, showed a significant positive gradient across the stenotic kidney, and markedly declined upon improvement of renal function were ox-LDL and TGF-β. Interestingly, however, ox-LDL was similarly elevated in the contralateral kidney vein and decreased with EPC delivery into the stenotic kidney, thus signaling between the two kidneys might have contributed to renal LDL oxidation. Contrarily, TGF-β showed a positive gradient, was elevated only in the stenotic kidney, and decreased with EPC. Pertinently, systemic TGF-β levels correlate with myocardial fibrosis and are involved in hypertrophic growth of cardiomyocytes under pressure overload [36], diastolic dysfunction, and cardiac hypertrophy [37]. Activation of TGF-β signaling contributes to myocardial fibrosis, as it stimulates fibroblasts and promotes their differentiation into myofibroblasts [38]. Therefore, TGF-β released from the stenotic kidney, possibly acting in concert with additional factors, is a likely mediator of distant cardiac remodeling in ARVD. IL-6 was also detectable in the stenotic kidney and completely restored by EPC, and might play an important role in cardiorenal signaling [39], but the small sample size and large variability impeded detection of statistically significant differences in its levels.

Importantly, declined circulating levels of biomarkers after improvement of renal function were accompanied by restored myocardial blood-flow and MP responses to cardiac challenge with adenosine, indicating improved microvascular function. MP is an important index of loss of microvascular integrity [8,40] and an early step in atherogenesis, which is often disclosed during challenge [8,15,17]. Blood pressure remained elevated in ARVD + EPC, because without correction of the stenosis, renal perfusion pressure (that triggers renin release) remained decreased, and because circulating levels of vasoconstrictor ET-1 [15] and isoprostanes [41] remained elevated.

ARVD also showed microvascular structural modifications. Microvascular rarefaction is frequently found in hypertension and ARVD, but was prevented in ARVD + EPC, and might have improved microvascular availability. Restoration of microvascular density could

be related to decreased ischemic episodes, downregulation of TGF-β [42], and amelioration of myocardial fibrosis, which in turn facilitates microvascular network development.

Hypertension and diastolic dysfunction are common in patients with CKD. Hypertension induces myocyte hypertrophy, interstitial fibrosis, and cardiac stiffness, which are implicated in impaired diastolic function (decreased E/A) and diastolic filling (decreased EDV). In this study, renal improvement by EPC improved cardiac diastolic function, likely by decreasing systemic levels of noxious humoral factors and thereby blunting myocardial fibrosis, cardiac stiffness, and LV hypertrophy, as well as indirectly via enhanced microvascular function and architecture.

Limitations

Our study was limited by the use of relatively young pigs, and ARVD duration was shorter than observed in patients. Nevertheless, declined kidney function had significant pathophysiological implications for evolution of cardiac injury. We cannot rule out partial contribution of systemic or local effects of EPC to cardiac improvement, but considering their negligible number detected in the myocardium this seems unlikely, especially given the rather large diminution in levels of circulating vasoconstrictors, inflammatory, and oxidative mediators. In addition, we cannot exclude the effect of changes in extracellular fluid volume or additional unknown factors linking renal function to myocardial microvascular dysfunction.

In summary, the present study shows that that deterioration of renal function in ARVD leads to release of mediators known to impair the remote myocardial microvascular integrity and structure. Selective improvement of renal function reduced circulating levels of inflammatory, oxidative, fibrogenic, and vasoactive factors, and thereby decreased myocardial fibrosis and enhanced microvascular integrity, architecture, and cardiac diastolic function. These salutatory benefits were conferred without any change in systemic arterial pressure or cholesterol levels. Therefore, this study underscores the crosstalk between the kidney and heart and implicates circulating mediators induced or released by dysfunctional kidneys in imposing functional and structural impairment in the remote myocardial microcirculation. Although the major source appears to be the prominently dysfunctional stenotic kidney, milder renal microvascular damage associated with hypertension and hypercholesterolemia, as observed in the contralateral kidney, may also lead to LDL oxidation. Hence, this study implies that correction of hypertension alone in patients with CKD may not suffice to abrogate cardiac impairment, and reinforces the need to improve renal function in order to decrease cardiovascular disease.

Acknowledgments

Source of funding

This study was partly supported by grant numbers DK-73608, DK77013, HL-77131, PO1HL-085307, and RR018898 from the NIH.

References

1. Coresh J, Selvin E, Stevens LA, et al. Prevalence of chronic kidney disease in the United States. JAMA. 2007; 298:2038–2047. [PubMed: 17986697]
2. James MTHB, Tonelli M. Early recognition and prevention of chronic kidney disease. Lancet. 2010:1296–1309. [PubMed: 20382326]
3. Culleton BF, Larson MG, Wilson PW, Evans JC, Parfrey PS, Levy D. Cardiovascular disease and mortality in a community-based cohort with mild renal insufficiency. Kidney International. 1999; 56:2214–229. [PubMed: 10594797]

4. Go AS, Chertow GM, Fan D, McCulloch CE, Hsu CY. Chronic kidney disease and the risks of death, cardiovascular events, and hospitalization. The New England Journal of Medicine. 2004; 351:1296–1305. [PubMed: 15385656]
5. Edwards MS, Craven TE, Burke GL, Dean RH, Hansen KJ. Renovascular disease and the risk of adverse coronary events in the elderly: a prospective, population-based study. Archives of Internal Medicine. 2005; 165:207–213. [PubMed: 15668368]
6. Shlipak MG, Fried LF, Crump C, et al. Elevations of inflammatory and procoagulant biomarkers in elderly persons with renal insufficiency. Circulation. 2003; 107:87–92. [PubMed: 12515748]
7. Chade AR, Brosh D, Higano ST, Lennon RJ, Lerman LO, Lerman A. Mild renal insufficiency is associated with reduced coronary flow in patients with nonobstructive coronary artery disease. Kidney International. 2006; 69:266–271. [PubMed: 16408115]
8. Lin J, Zhu X, Chade AR, et al. Monocyte chemoattractant proteins mediate myocardial microvascular dysfunction in swine renovascular hypertension. Arteriosclerosis, Thrombosis, and Vascular Biology. 2009; 29:1810–1816.
9. Chade AR, Zhu X, Lavi R, et al. Endothelial progenitor cells restore renal function in chronic experimental renovascular disease. Circulation. 2009; 119:547–557. [PubMed: 19153272]
10. Chade AR, Zhu XY, Krier JD, Jordan KL, Textor SC, Grande JP, et al. Endothelial progenitor cells homing and renal repair in experimental renovascular disease. Stem Cells. 2010; 28:1039–1047. [PubMed: 20506499]
11. Chade AR, Rodriguez-Porcel M, Grande JP, et al. Distinct renal injury in early atherosclerosis and renovascular disease. Circulation. 2002; 106:1165–1171. [PubMed: 12196346]
12. Lerman LO, Schwartz RS, Grande JP, Sheedy PF, Romero JC. Noninvasive evaluation of a novel swine model of renal artery stenosis. Journal of the American Society of Nephrology. 1999; 10:1455–1465. [PubMed: 10405201]
13. Boggia J, Li Y, Thijs L, et al. Prognostic accuracy of day versus night ambulatory blood pressure: a cohort study. Lancet. 2007; 370:1219–1229. [PubMed: 17920917]
14. Daghini E, Primak AN, Chade AR, et al. Evaluation of porcine myocardial microvascular permeability and fractional vascular volume using 64-slice helical computed tomography (ct). Investigative Radiology. 2007; 42:274–282. [PubMed: 17414522]
15. Rodriguez-Porcel M, Herrman J, Chade AR, et al. Long-term antioxidant intervention improves myocardial microvascular function in experimental hypertension. Hypertension. 2004; 43:493–498. [PubMed: 14718362]
16. Zhu XY, Daghini E, Chade AR, et al. Simvastatin prevents coronary microvascular remodeling in renovascular hypertensive pigs. Journal of the American Society of Nephrology. 2007; 18:1209–1217. [PubMed: 17344424]
17. Zhu XY, Daghini E, Chade AR, et al. Role of oxidative stress in remodeling of the myocardial microcirculation in hypertension. Arteriosclerosis, Thrombosis, and Vascular biology. 2006; 26:1746–1752.
18. Rodriguez-Porcel M, Lerman A, Herrmann J, et al. Hypertension exacerbates the effect of hypercholesterolemia on the myocardial microvasculature. Cardiovascular Research. 2003; 58:213–221. [PubMed: 12667964]
19. Zhu XY, Daghini E, Rodriguez-Porcel M, et al. Redox-sensitive myocardial remodeling and dysfunction in swine diet-induced experimental hypercholesterolemia. Atherosclerosis. 2007; 193:62–69. [PubMed: 16996066]
20. Zhu XY, Rodriguez-Porcel M, Bentley MD, et al. Antioxidant intervention attenuates myocardial neovascularization in hypercholesterolemia. Circulation. 2004; 109:2109–2115. [PubMed: 15051643]
21. Cuocolo A, Sax FL, Brush JE, Maron BJ, Bacharach SL, Bonow RO. Left ventricular hypertrophy and impaired diastolic filling in essential hypertension. Diastolic mechanisms for systolic dysfunction during exercise. Circulation. 1990; 81:978–986. [PubMed: 2137735]
22. Valle Gottlieb MG, da Cruz IB, Duarte MM, et al. Associations among metabolic syndrome, ischemia, inflammatory, oxidatives, and lipids biomarkers. The Journal of Clinical Endocrinology and Metabolism. 2010; 95:586–591. [PubMed: 20016051]

23. Suwaidi JA, Hamasaki S, Higano ST, Nishimura RA, Holmes DR Jr, Lerman A. Long-term follow-up of patients with mild coronary artery disease and endothelial dysfunction. Circulation. 2000; 101:948–954. [PubMed: 10704159]
24. McAlister FA, Ezekowitz J, Tonelli M, Armstrong PW. Renal insufficiency and heart failure: prognostic and therapeutic implications from a prospective cohort study. Circulation. 2004; 109:1004–1009. [PubMed: 14769700]
25. Wali RK, Wang GS, Gottlieb SS, et al. Effect of kidney transplantation on left ventricular systolic dysfunction and congestive heart failure in patients with end-stage renal disease. Journal of the American College of Cardiology. 2005; 45:1051–1060. [PubMed: 15808763]
26. London GM, Marchais SJ, Guerin AP, Metivier F, Adda H, Pannier B. Inflammation, arteriosclerosis, and cardiovascular therapy in hemodialysis patients. Kidney International Supplement. 2003:S88–S93. [PubMed: 12694318]
27. Ronco C, Cruz DN, Ronco F. Cardiorenal syndromes. Current Opinion in Critical Care. 2009; 15:384–391. [PubMed: 19542883]
28. Eirin A, Zhu XY, Urbieta-Caceres VH, et al. Persistent kidney dysfunction in swine renal artery stenosis correlates with outer cortical microvascular remodeling. American Journal of Physiology. 2011; 300:F1394–F1401. [PubMed: 21367913]
29. Lerman LO, Nath KA, Rodriguez-Porcel M, et al. Increased oxidative stress in experimental renovascular hypertension. Hypertension. 2001; 37:541–546. [PubMed: 11230332]
30. Xu J, Carretero OA, Liao TD, Peng H, Shesely EG, Xu J, et al. Local angiotensin ii aggravates cardiac remodeling in hypertension. American Journal of Physiology Heart and Circulatory Physiology. 2010; 299:H1328–H1338. [PubMed: 20833959]
31. Brown NJ. Aldosterone and end-organ damage. Current Opinion in Nephrology and Hypertension. 2005; 14:235–241. [PubMed: 15821416]
32. Barton M. Reversal of proteinuric renal disease and the emerging role of endothelin. Nature Clinical Practice. 2008; 4:490–501.
33. Shigematsu Y, Hamada M, Okayama H, et al. Left ventricular hypertrophy precedes other target-organ damage in primary aldosteronism. Hypertension. 1997; 29:723–727. [PubMed: 9052887]
34. Helmersson J, Basu S. F2-isoprostane excretion rate and diurnal variation in human urine. Prostaglandins, Leukotrienes, and Essential Fatty Acids. 1999; 61:203–205.
35. Bellomo G, Venanzi S, Verdura C, Saronio P, Esposito A, Timio M. Association of uric acid with change in kidney function in healthy normotensive individuals. American Journal of Kidney Diseases. 2010; 56:264–272. [PubMed: 20385436]
36. Villar AV, Cobo M, Llano M, et al. Plasma levels of transforming growth factor-beta1 reflect left ventricular remodeling in aortic stenosis. PLoS One. 2009; 4:e8476. [PubMed: 20041033]
37. Kuwahara F, Kai H, Tokuda K, et al. Transforming growth factor-beta function blocking prevents myocardial fibrosis and diastolic dysfunction in pressureoverloaded rats. Circulation. 2002; 106:130–135. [PubMed: 12093782]
38. Sovari AA, Dudley SC. Using serum transforming growth factor-beta to predict myocardial fibrosis. Circulation Research. 2010; 106:e3. author reply e4. [PubMed: 20203307]
39. Melendez GC, McLarty JL, Levick SP, Du Y, Janicki JS, Brower GL. Interleukin 6 mediates myocardial fibrosis, concentric hypertrophy, and diastolic dysfunction in rats. Hypertension. 2010; 56:225–231. [PubMed: 20606113]
40. Antonios TF. Microvascular rarefaction in hypertension–reversal or overcorrection by treatment? American Journal of Hypertension. 2006; 19:484–485. [PubMed: 16647619]
41. Krier JD, Rodriguez-Porcel M, Best PJ, Romero JC, Lerman A, Lerman LO. Vascular responses in vivo to 8-epi pgf(2alpha) in normal and hypercholesterolemic pigs. American Journal of Physiology Regulatory, Integrative and Comparative Physiology. 2002; 283:R303–R308.
42. Hoot KE, Oka M, Han G, Bottinger E, Zhang Q, Wang XJ. Hgf upregulation contributes to angiogenesis in mice with keratinocyte-specific smad2 deletion. The Journal of Clinical Investigation. 2010; 120:3606–3616. [PubMed: 20852387]

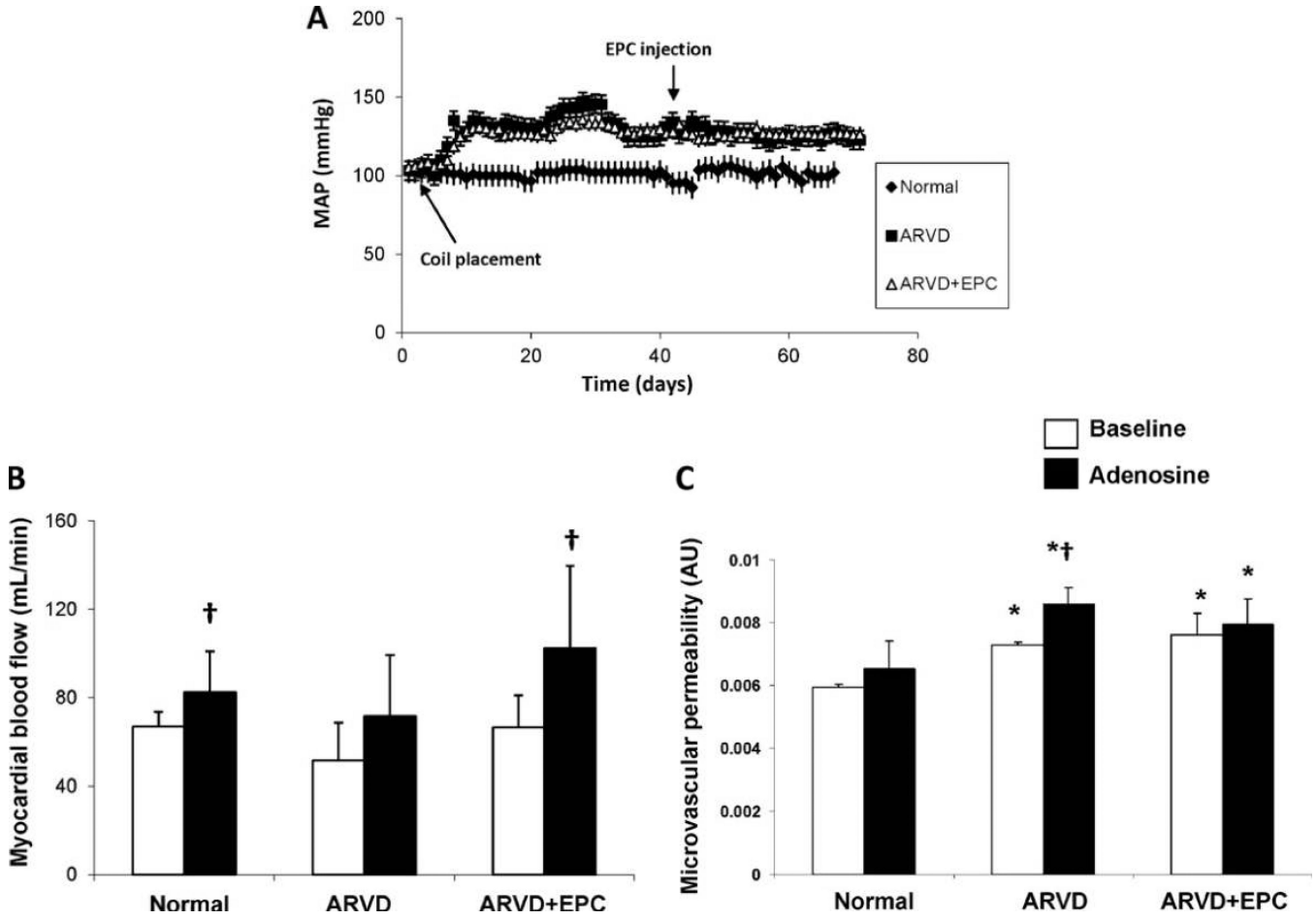

Figure 1.

(A) Changes in mean arterial pressure (MAP) over time in normal, ARVD, and ARVD + EPC pigs (n = 5–6/group). EPC infusion had no effect on MAP in ARVD. (B) and (C) Myocardial blood-flow (ml/min) and microvascular permeability (MP, arbitrary units: AU) obtained using fast-CT in the anterior-wall in normal, atherosclerotic renovascular-disease (ARVD) and ARVD + endothelial progenitor cells (ARVD + EPC) pigs. Basal anterior-wall myocardial MP increased in ARVD and ARVD + EPC. Adenosine disclosed impaired MP responses in ARVD, which were preserved in ARVD + EPC. *$p \leq 0.05$ vs. normal, $^{\dagger}p \leq 0.05$ vs. baseline.

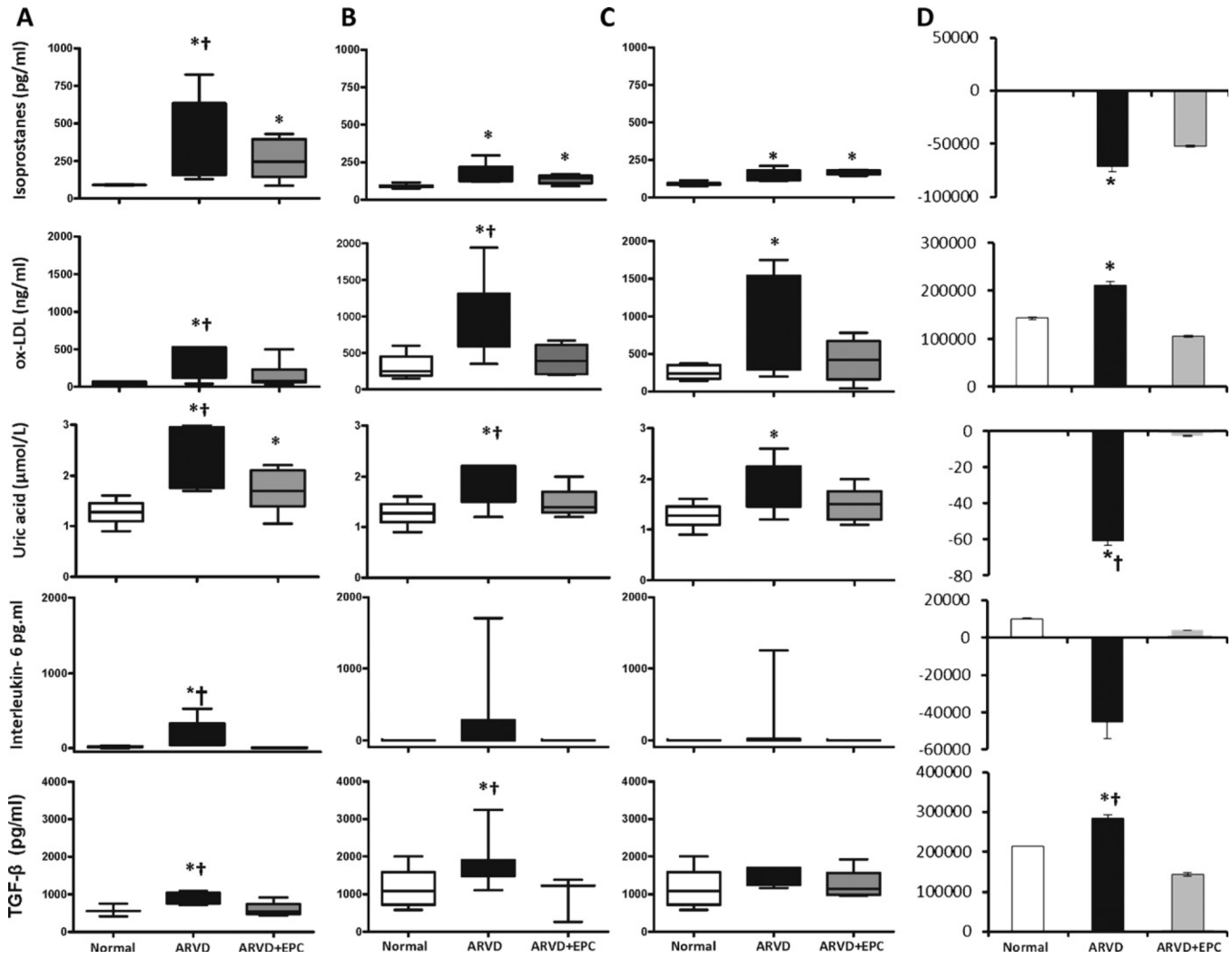

Figure 2.

Oxidative mediators PGF2α-isoprostanes, uric-acid, and oxidized (ox)-LDL, inflammatory interleukine-6, and the fibrogenic TGF-β in normal, ARVD and ARVD + EPC in the systemic circulation (A), and veins of the stenotic (B) and ontralateral (C) kidneys. (D) Respective gradients across the stenotic kidney. *$p \leq 0.05$ vs. normal, †$p \leq 0.05$ vs. ARVD + EPC.

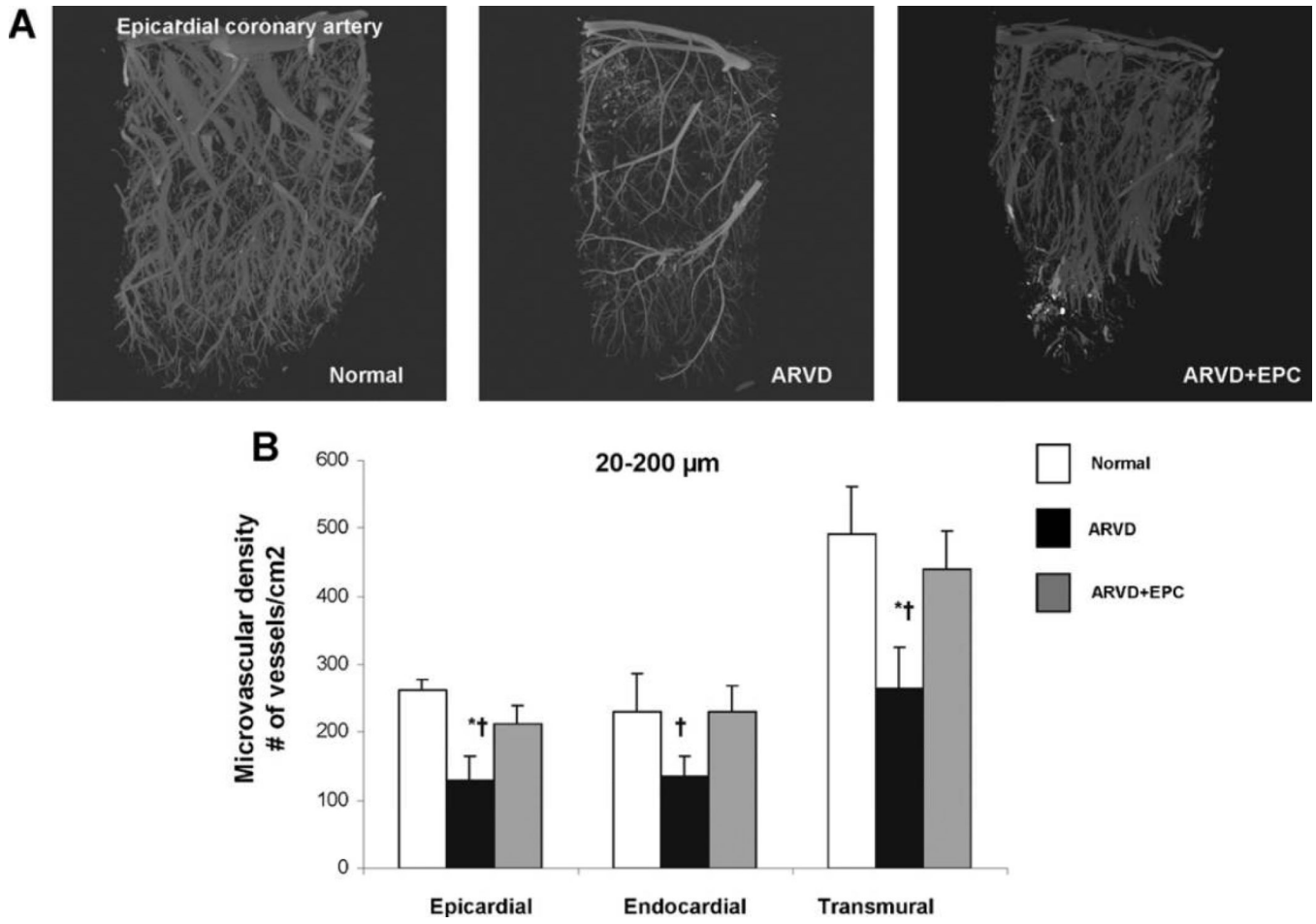

Figure 3.

Myocardial microvascular density assessed by micro-CT in normal, atherosclerotic renovascular-disease (ARVD) and ARVD + endothelial progenitor cells (ARVD + EPC). (A) Representative micro-CT images of myocardial microvessels. (B) Quantitation of microvascular density. The transmural density of microvessels (20–200 µm in diameter) in normal (white-bars) decreased in ARVD (black-bars) and was preserved in ARVD + EPC (gray-bars). *$p \leq 0.05$ vs. normal, $^{\dagger}p \leq 0.05$ vs. ARVD + EPC.

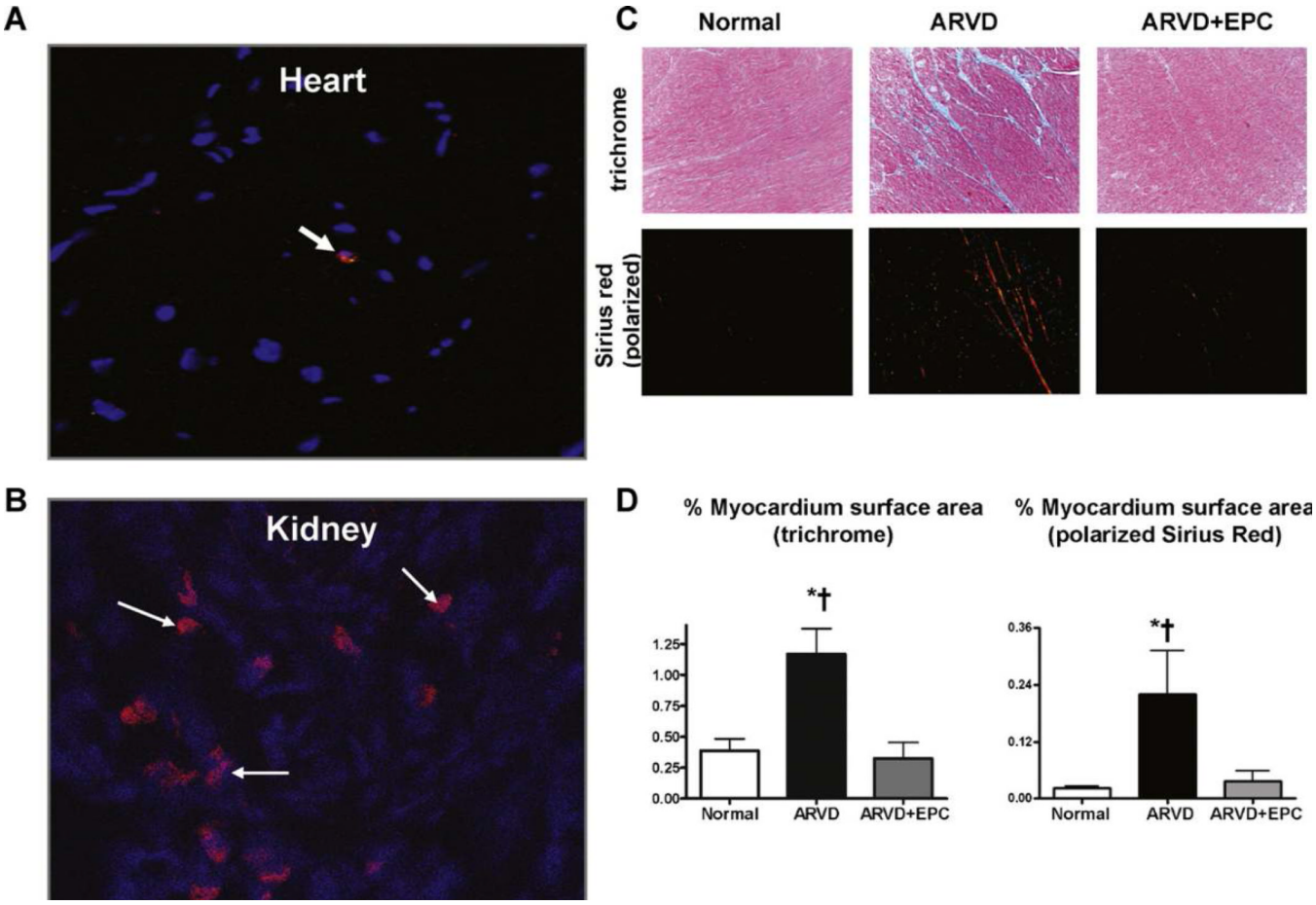

Figure 4.

Representative immunofluorescence staining of CM-DiI (red) in frozen heart (A) and kidney (B) sections of ARVD + EPC (both 20×). (C) Representative myocardial trichrome (blue, 20×) and Sirius-red (polarized light, red, 20×) staining for myocardial fibrosis and quantitation (D) in the normal, ARVD and ARVD + EPC. Myocardial fibrosis in ARVD decreased after improvement of renal function. *$p \leq 0.05$ vs. normal and $^{\dagger}p \leq 0.05$ vs. ARVD + EPC.

Table 1

General characteristics and cardiac function in normal, chronic atherosclerotic renovascular-disease (ARVD) and ARVD + endothelial progenitor cells (ARVD + EPC) pigs.

	Normal	ARVD	ARVD + EPC
n	6	6	6
Body weight (kg)	50±1	54±3	52±4
Degree of Stenosis (%)		81±8*	74±7*
Total cholesterol (mg/dl)	77±3	410±39*	373±44*
Systemic PRA (ng/ml/h)	0.21±0.02	0.17±0.02	0.14±0.02
Mean arterial pressure (mmHg)	101±7	127±6*	126±5*
Systolic pressure (mmHg)	124±10	155±12*	159±11*
Diastolic pressure (mmHg)	79±6	101±7*	98±9*
Daytime pressure (mmHg)	118±9	142±11*	148±±13*
Nighttime pressure (mmHg)	91±5	120±8*	119±9*
Creatinine (ml/dl)	1.4±0.06	1.7±0.14	1.5±0.15
Urine protein (_g/ml)	22±4	32±4	30±3
Stroke volume (ml)	54±5	46±3	48±5
Cardiac output (l/min)	3.6±0.4	3.1±0.1	3.5±0.5
Early/late LV filling (E/A)	1.85±0.10	0.90±0.15*,†	1.27±0.08*
LVMM (gr)	1.90±0.10	3.20±0.30*,†	2.40±0.20*
End-diastolic volume (cc)	188.6±18.5	133.2±13.2*	146.3±14.7
Aldosterone (pg/ml)	683.75±68	1131.43±258*,†	697.85±116
Endothelin-1 (pg/ml)	3.90±0.08	4.90±0.17*,†	4.4±0.13*
TNFα (pg/ml)	43±3.5	142±7*,†	90±4.5*

PRA: plasma renin activity; GFR: glomerular filtration rate; LVMM: left ventricular muscle mass.

*$p < 0.05$ vs. normal.

†$p < 0.05$ vs. ARVD + EPC.

Table 2

Renal hemodynamics and function in normal, chronic atherosclerotic renovascular-disease (ARVD) stenotic and contralateral kidneys with or without EPC treatment.

	Normal	ARVD		ARVD + EPC	
		Stenotic	Contralateral	Stenotic	Contralateral
n	6	6	6	6	6
Volume (cc)	124.6±3.7	84.1±10.1 *	136.7±7.7 ≠	96.1±5.9	117.0±4.9 ≠
GFR (ml/min/cc)	0.72±0.12	0.50±0.07 *,†	0.80±0.02 ≠	0.80±0.12	0.78±0.07
GFR (ml/min)	70.3±2.1	56.4±8.8 *,†	92.4±4.0 *,≠	74.4±5.9	87.4±4.8
Renal blood flow (ml/min)	581.4±15.1	311.1±59.8 *,≠	545.3±72.9 ≠	403.5±19.9	537.0±37.9 ≠
Perfusion (ml/min/cc)	4.9±0.1	3.7±0.4 *	4.3±0.3	4.3±0.3	4.6±0.2

GFR: glomerular filtration rate.

* $p < 0.05$ vs. normal.

† $p < 0.05$ vs. ARVD + EPC.

≠ $p < 0.05$ vs. stenotic kidney.